한국광물학회지 제 18 권 제 3 호 (2005년 9월)
J. Miner. Soc. Korea, 18(3), 227-236 (September, 2005)

Chemical Characterization of Oscillatory Zoned Tourmaline from Diaspore Nodule, an Aluminum-rich Clay Deposit, Milyang, South Korea

밀양 고알루미나 점토광상 다이아스포아 단괴내의 진동누대 전기석의 화학적 특징

Chang Oh Choo (추 창 오) · Yeongkyoo Kim (김 영 규)*

Department of Geology, Kyungpook National University, Daegu, Korea
(경북대학교 자연과학대학 지질학과)

ABSTRACT : Hydrothermal tourmaline occurs as aggregates or dissemination in the diaspore nodule from an aluminum-rich clay deposit, Milyang, southeastern Korea. Most crystals of tourmaline show complex textures that are finely zoned. The fine-scale chemical zonation of hydrothermal tourmaline reflects the fluctuation conditions that would be expected from fluid mixing in open systems. Oscillatory chemical zoning in tourmaline formed and showed similar patterns, regardless of its crystallographic directions. Mg was enriched in the early stage of crystal growth while Fe was enriched in the later stage, with fluctuations of the ratio of Fe to Mg. Chemical analysis, BSE images, and X-ray compositional maps confirm that the oscillatory zoning in tourmaline is exclusively controlled by the variations of Fe and Mg contents, but the contribution of boron to the zonation is insignificant. The fact that tourmaline altered to diaspore and dickite indicates that tourmaline was unstable with respect to these aluminous minerals as the B, Fe, and Mg activities decreased. Therefore, the aluminum activity may control the stability of tourmaline in the hydrothermal system.

Key words : tourmaline, diaspore nodule, oscillatory zoning, aluminum activity

요약 : 밀양점토광상의 알루미늄이 풍부한 다이아스포아 단괴에서 열수변질 기원 전기석은 집합체나 미립으로 산출한다. 대부분의 전기석 결정은 미세한 대구조가 특징적인데, 이는 열수변질 작용동안 개방계의 유체혼합과 같은 변동이 심한 환경에서 형성되었음을 지시한다. 본 전기석의 화학적 진동누대 구조의 양상은 결정축의 방향과는 무관하게 흡사한 특징을 보인다. Mg는 결정성장 초기, Fe는 후기 단계동안에 부화되었으며, Fe/Mg의 비는 규칙적으로 진동함을 보여 준다. 화학분석, 후방산란영상(BSE), X-선 화학분석도에 따르면 전기석내 진동누대구조는 Fe와 Mg 함량변화에 주로 제어되었으며 붕소함량의 기여도는 미미하다. 전기석이 다이아스포아와 딕카이트로 변질되는 것으로 볼 때 전기석은 B, Fe, Mg의 활동도가 감소하면서 이들 고알루미나 광물에 비하여 불안정해 진다. 그러므로 열수계내 알루미늄 활동도가 전기석의 안정성을 제어하는 것으로 볼 수 있다.

주요어 : 전기석, 다이아스포아 단괴, 진동누대구조, 알루미늄 활동도

*교신저자: ygkim@knu.ac.kr

INTRODUCTION

Tourmaline, developed as a consequence of infiltration of B-bearing hydrothermal fluids, can have a wide range of compositions that are a function of the compositions of the altering host rock and the invasive fluid (Cavarretta and Puxeddu, 1990) and has long been recognized as an important gangue mineral in various hydrothermal ore deposits (Taylor and Slack, 1984; Slack, 1996). Tourmaline, $XY_3Z_6(BO_3)3Si_6O_{18}$ (O, OH) (OH, F), shows many possible substitutions between end-members (Henry and Dutrow, 1996). The X site is occupied predominantly by Na and Ca in the nine-fold coordination but may also be vacant. The Y and Z sites are both octahedrally coordinated; divalent cations are incorporated preferentially into the Y site, whereas Al_3 + generally enters the smaller Z site. The wide range of variation in the chemical composition of tourmaline has attracted much attention because it has the potential to provide insight into local chemical environment and compositional evolution of fluid influx as well as igneous and metamorphic rocks (London and Manning, 1995; Dutlow and Henry, 2000). Moreover, the tourmaline group is characterized by complex oscillatory zoning and compositionally diverse members (Taylor and Slack, 1984; Michailidis *et al.*, 1996; Henry *et al.*, 1999; Choo *et al.*, 2001).

Tourmaline occurs in the diaspore nodules formed in the Milyang clay deposit, southeastern Korea (Kim *et al.*, 1992). This aluminum-rich deposit characterized by predominant dickite, diaspore, and pyrophyllite with trace tourmaline and dumortierite is known to have formed by hydrothermal alteration of late Cretaceous andesitic tuff, possibly associated with subsequent granite intrusion. Mineralogical studies on fine textures and chemistry of tourmaline in association with aluminous minerals are important to better explain the formation condition of hydrothermal clays (e.g., Choo and Kim, 2003). Especially, an understanding of the causes of oscillatory zoning is essential to the elucidation of formation conditions of hydrothermal minerals as well as physicochemical processes of magma evolution (Shore and Fowler, 1996). So far, little is known about mineralogical features of tourmaline formed in the diaspore nodule. The occurrence of tourmaline in the diaspore nodule associated with aluminum-rich clays has been less commonly encountered worldwide. The aims of the present study are to interpret the patterns of chemical zoning in tourmaline and to discuss its stability with respect to aluminous minerals in the diaspore nodule.

GEOLOGY AND SAMPLES

In the southeastern part of Korea, several clay deposits have been formed by hydrothermal alteration of late Cretaceous Yucheon volcanic rocks that are in a close association with distribution of the Bulguksa Granite of late Cretaceous to early Tertiary in age. Acidic hydrothermal alteration resulted in the formation of dickite, pyrophyllite, and illite-rich clay deposits. Interestingly, diaspore nodules frequently occur in the Milyang clay deposit (Lat.35° 30′N-35° 32′N and Long. 128° 41′ E-128° 47E). The clay deposit is predominantly composed of dickite and pyrophyllite, with accessory minerals such as diaspore, quartz, tosudite, illite, tourmaline, dumortierite, wavellite, barite, and pyrite (Kim *et al.*, 1992; Lee *et al.*, 1993; Koh *et al.*, 2000; Choo *et al.*, 2001). In the Milyang mine area, the host rocks consist of andesitic tuff interlayered in the aphanitic andesite belonging to the Yucheon volcanic group of late Cretaceous age, which are characterized by calc-alkaline series occurred at the volcanic arc environment in continental margin (Hwang and Kim, 1994). The ages of the Yucheon volcanic rocks are known to be 75～64 Ma (Min *et al.*, 1982). The andesitic tuff has a main bedding plane of N60E and 20NW with some irregular variations, mostly consisting of plagioclase, hornblende, chlorite, opaque minerals, and rock fragments. Biotite granite around the andesitic tuff is found as the only important intrusive rock and is composed of quartz, biotite, orthoclase, plagioclase, and hornblende. The biotite granite with ages 66.5 ～62 Ma was derived from I-type magma with

calc-alkaline series (Hong and Choi, 1988; Jin *et al.*, 1991). The dickite- and pyrophyllite- rich clay ore is developed as a lens-like form or massive body in the andesitic tuff, and the diaspore nodules occur along or near the fractured zones developed in the clay body. Contact boundary between the diaspore nodule and the clays is relatively sharp, but rarely gradational. The diaspore nodules are well-rounded spherical or ellipsoidal in shape, ranging from 0.5 cm to 15 cm in diameter, mostly 5～10 cm. It consists mostly of equigranular platy diaspore, displaying no radial structure. Dark tourmaline occurs as aggregates or dissemination in the diaspore nodule. Papezik and Keats (1976) documented the diaspore nodule in the pyrophyllite deposit formed in rhyolite flows and pyroclastics.

ANALYTICAL METHODS

Mineral identification and chemical analysis on the diaspore nodules were done using X-ray diffractometer (XRD). XRD analyses of bulk nodule samples were carried out for identification of constituent minerals using a Rigaku Geigerflex RAD3-C with Ni-filtered CuKα radiation. The XRD data were recorded at 40 kV and 30 mA by counting 3 seconds at steps of 0.02° 2θ, from 5 to 65° 2θ. Electron microprobe analysis (EMPA) was performed on polished thin sections using Cameca SX51 microprobe and Shimazu 1600 electron microprobe. Quantitative chemical analysis was done by EMPA fitted with automated wavelength-dispersive spectrometer (WDS) operated at 1 μm beam diameter, 15 kV accelerating voltage and 10 nA beam current. Chemical results were calculated using a ZAF correction and Fe was assumed as ferrous, and cation numbers were normalized on the basis of 29 oxygens. Due to analytical limitations for boron by EMPA, B was calculated based on the assumption of 3 B atoms per formula unit, which makes it possible to calculate the weight % of B_2O_3 necessary to produce 3 B cations (Henry and Dutrow, 1996; Henry *et al.*, 1999). Such assumptions could yield satisfactory data when analyzing borosilicates such as tourmaline (Werding and Schreyer, 1996). For quantitative analyses the point scanning on zoned tourmaline crystals was performed at the interval of 2 μm. Line scanning at 0.08 μm step per second was made across the zoned crystals for semi-quantitative analyses of B, Fe, and Mg contents in order to compare chemical variation as a function of crystallographic axis. Backscattered electron (BS E) images and X-ray maps of atomic distribution were also obtained from the polished thin sections.

RESULTS

Occurrence and Texture of Tourmaline in the Diaspore Nodule

Based on XRD and BSE images, the diaspore nodule consists mostly of diaspore, with small amount of dickite, pyrophyllite, tourmaline, wavellite, anatase, barite, celestine, and pyrite. Tourmaline is commonly associated with prismatic or lath-shaped diaspore that occurs as the largest crystal with 0.1～2 mm in length. It is also found with dickite occurring as fine aggregates or a book-stacking texture. Radiating aggregates of tourmaline are found in the diaspore nodule, and less commonly, disseminated tourmaline is also encountered (Fig. 1). Tourmaline altered to dickite at the marginal part of the crystal and diaspore also partly altered to dickite.

Chemistry and Oscillatory Zoning Pattern of Tourmaline

Tourmaline reveals complex zonal textures under BSE images (Fig. 2). Oscillatory zoning in the tourmaline crystals is discernable, although there is a general trend of Mg-rich core and Fe- rich rim. Oscillation bands are relatively straight and involve a larger compositional range. Delicate growth zones as thin as 1 μm are easily observed in compositional zones. The oscillation patterns are often interrupted by a change in the mode of oscillations or another style of crystal growth. Especially rounded faces or trigonal faces developed in the inner part of the

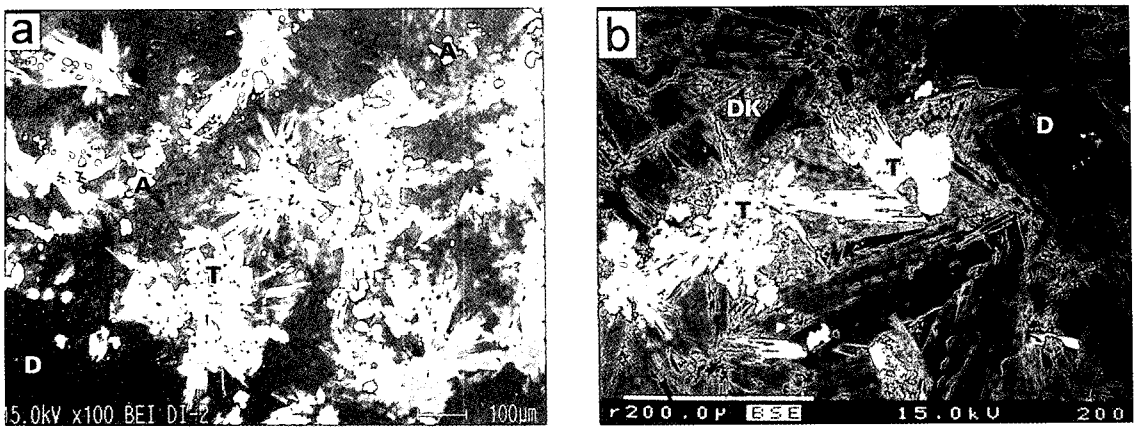

Fig. 1. Backscattered electron (BSE) images of constituent minerals in the diaspore nodule. (a) Radiating aggregates of tourmaline in the diaspore matrix. (b) Lath-shaped diaspore and dickite. Symbol; A: anatase, D: diaspore, DK; dickite, T: tourmaline. Scales are 100 μm for (a) and 200 μm for (b), respectively.

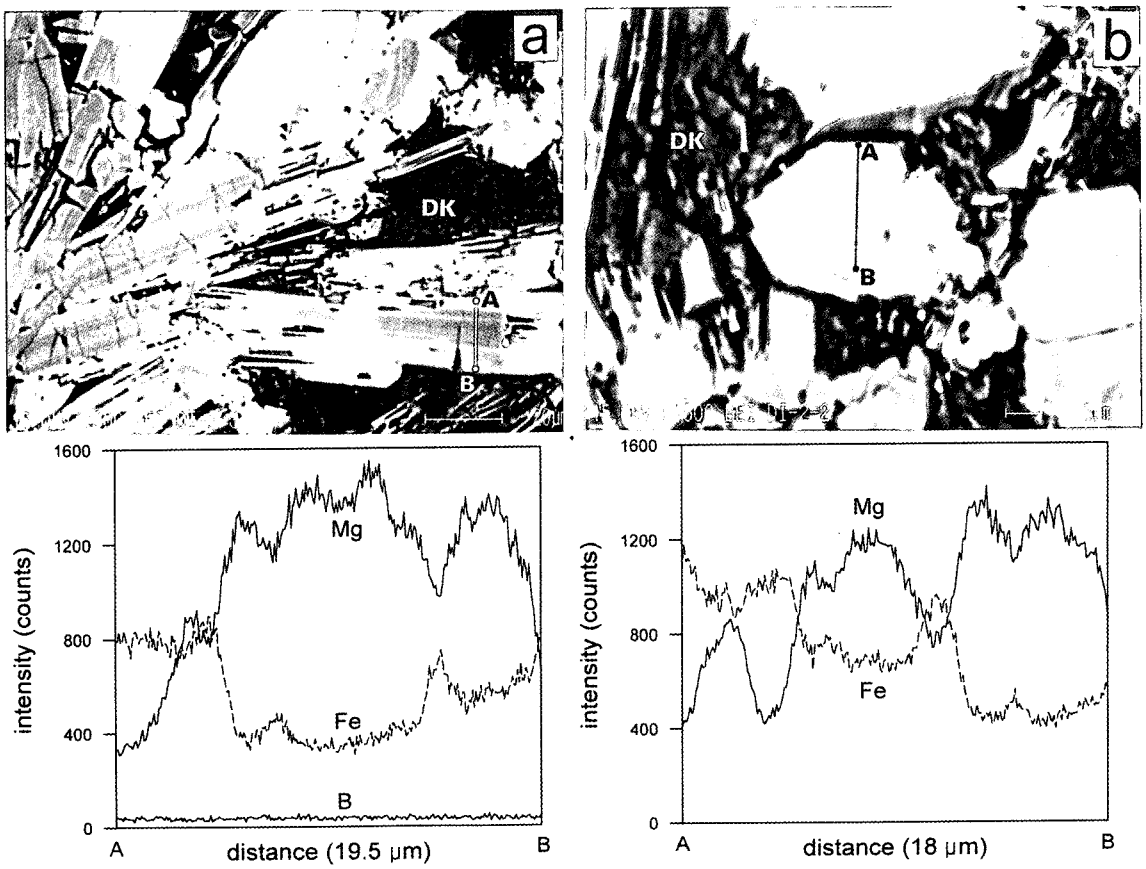

Fig. 2. BSE images of tourmaline and compositional profiles across the oscillatory zoning with alternating Fe-rich band (bright grey) and Mg-rich band (dark grey). DK refers to dickite. (a) Line scanning along the A-B line on the crystal cut parallel to the c-axis. Scale is 20 μm. (b) Line scanning along the A-B line in the crystal cut perpendicular to the c-axis of finely zoned tourmaline. Scale is 5 μm.

crystal appear to evolve gradually to hexagonal or pseudo-hexagonal faces towards the outer rim of tourmaline crystals. X-ray maps of oscillatory-zoned tourmaline also show that Mg is enriched in the core, whereas Fe is enriched in the rim, consistent with the compositional contrast of the BSE images. It is clear that alternation of Fe-rich band and Mg-rich band is the most important factor that controls the oscillatory zoning pattern.

EMPA data were obtained from the outermost rim toward the inner core in the oscillatory- zoned tourmaline, using point scanning across the A-B lines in Fig. 2. As illustrated in Table 1, tourmaline is classified as schorl-dravite series in chemical composition, that is, ferridravite. Fe and Mg are the most important components responsible for the oscillatory zoning, whereas SiO_2 and Al_2O_3 generally exhibit little variations across the zoned area. It is evident that Na component is also fluctuated across the zoning area, but its contribution to the zoning pattern may be negligible due to its very low content. There are recognizable deficiencies in the X- and Y-sites, respectively. The B_2O_3 contents, though assumed as ideal, are nearly constant across the oscillatory zoned crystal, which indicates its little contribution to the zoning development.

Oscillatory zoning patterns with respect to the crystallographic axes are comparable using line-scanned profiles. For instance, compositional profiles of oscillatory zoning were obtained from line scanning along A-B lines on the tourmaline crystals cut parallel to the c-axis (Fig. 2a) and perpendicular to the c-axis (Fig. 2b), respectively. Fine growth lamellae associated with Fe and Mg contents are seen along and normal to the c-axis. Consequently, it is likely that oscillatory chemical zoning in tourmaline can be formed, regardless of its crystallographic directions. Oscillatory-zoned tourmaline yields very similar zoning patterns when viewed in both directions mentioned above. Notably, Mg is enriched in the early stage of crystal growth while Fe is enriched in the later stage, with fluctuations of the ratio of Fe to Mg (Fig. 3). It is obvious that boron shows nearly the same content, indicating that it has little effect on development of the oscillatory zoning. This finding is consistent with the EPMA result showing that B_2O_3 contents are nearly constant across the zoned tourmaline, as illustrated in Table 1.

Fairly good correlations between some elements are found in oscillatory tourmaline (Fig. 4). The plot (Si + Mg + Fe) vs. total Al yields a negative linear relation with high determinative coefficient, R2 = 0.98, suggesting an Fe-Tschermak substitution. Werding and Schreyer (1996) showed the Tschermak substitution with total Al for (Si + Mg) using electron microprobe data obtained from synthetic dravite. In the oscillatory tourmaline, Fe-Tschermak substitution may be due to the presence of Fe- and Mg-rich tourmaline in a close association with Al-rich minerals such as diaspore and dickite. The plot of Fe vs. Mg is negatively lineated with R2 = 0.87 showing a good substitution relationship. The plot of Na/(Na + Ca) vs. Al in the Y-site exhibits fairly a good substitution relation with R2 = 0.84. Though its content is very low, the Ca content increases with increasing total Al content with R2 = 0.91. Apart from these, correlations between chemical components are insignificant. Although more chemical analyses are needed to confirm its validity, Al appears to have a compositional gap in oscillatory zoning because there is a missing range in chemical compositions. Significant variation in the Fe/(Fe + Mg) ratio is revealed across the oscillatory-zoned area in tourmaline, ranging from 0.34 to 0.86, which is comparable to tourmalines from other geologic setting. In general, tourmaline from Li-poor granites have high average Fe/(Fe + Mg) ratio of more than 0.85 (Power, 1968; Nieva, 1974), but one from massive sulfide environments shows very low, with an average Fe/(Fe + Mg) ratio of 0.21 (Taylor and Slack, 1984). The Fe/(Fe + Mg) ratio reveals a gradual increase from the core to the rim with the concentrations of Fe and Mg fluc--tuated. The variations in vacancy of the X-site are remarkably compared to those of Y-sites that show weak variation. It appears that Al in the Y-site generally decreases from the core with fluctuation, but the decreasing magnitude is relatively small. Na, an exclusively dominant cation in the X-site, shows

Table 1. Chemical analyses for zoned tourmaline. Point scanning with 2 μm step was made by EPMA across the A-B line in Fig. 3

	point A (outer rim)	DI-1	DI-2	DI-3	DI-4	DI-5	DI-6	DI-7	DI-8	point B (inner core)
SiO_2	35.14	35.95	35.66	35.94	36.31	36.44	36.59	36.63	35.51	34.73
TiO_2	0.12	0.09	0.11	0.08	0.07	0.10	0.13	0.08	0.05	0.10
$B2O_3$*	10.36	10.48	10.46	10.48	10.59	10.58	10.65	10.85	10.38	10.45
Al_2O_3	34.32	34.61	34.05	34.46	34.44	33.59	34.82	37.60	35.70	36.19
FeO**	13.10	10.63	10.89	12.24	9.38	8.66	11.09	5.71	4.33	5.10
MgO	1.19	2.43	2.66	1.64	3.64	4.43	2.36	4.10	4.71	4.79
MnO	0.03	0.04	0.05	0.10	0.04	0.01	0.01	0.03	0.00	0.00
CaO	0.04	0.03	0.02	0.03	0.02	0.02	0.03	0.08	0.08	0.09
Na_2O	1.06	0.99	1.22	1.04	1.22	1.42	1.17	1.20	0.61	1.18
K_2O	0.00	0.00	0.00	0.00	0.00	0.00	0.00	0.00	0.01	0.01
Total (wt.%)	95.35	95.25	95.12	95.99	95.71	95.24	96.85	96.28	91.37	92.64
				Structural formulae based on 29 oxygens						
B	3.00	3.00	3.00	3.00	3.00	3.00	3.00	3.00	3.00	3.00
Si	5.90	5.96	5.93	5.96	5.96	5.99	5.97	5.86	5.95	5.77
AlT	0.10	0.04	0.07	0.04	0.04	0.01	0.03	0.14	0.05	0.23
Total Z-site	6.00	6.00	6.00	6.00	6.00	6.00	6.00	6.00	6.00	6.00
Al_Y	0.69	0.73	0.61	0.70	0.62	0.50	0.67	0.95	1.01	0.86
Ti	0.02	0.01	0.01	0.01	0.01	0.01	0.02	0.01	0.01	0.01
Fe_2^+	1.84	1.47	1.52	1.70	1.29	1.19	1.51	0.76	0.61	0.71
Mg	0.30	0.60	0.66	0.40	0.89	1.08	0.57	0.98	1.18	1.19
Mn	0.00	0.01	0.01	0.01	0.01	0.00	0.00	0.00	0.00	0.00
Total Y-site	2.84	2.82	2.81	2.82	2.81	2.79	2.78	2.70	2.80	2.77
Ca	0.01	0.01	0.00	0.00	0.00	0.00	0.01	0.01	0.01	0.02
Na	0.35	0.32	0.39	0.33	0.39	0.45	0.37	0.37	0.20	0.38
K	0.00	0.00	0.00	0.00	0.00	0.00	0.00	0.00	0.00	0.00
Total X-site	0.35	0.33	0.40	0.34	0.39	0.46	0.38	0.39	0.21	0.40
Fe/(Fe+Mg)	0.86	0.71	0.70	0.81	0.59	0.52	0.72	0.44	0.34	0.37
Na/(Na+Ca)	0.98	0.98	0.99	0.99	0.99	0.99	0.99	0.97	0.94	0.96

* Calculated using stoichiometric constraints.

** Assumed total iron as FeO.

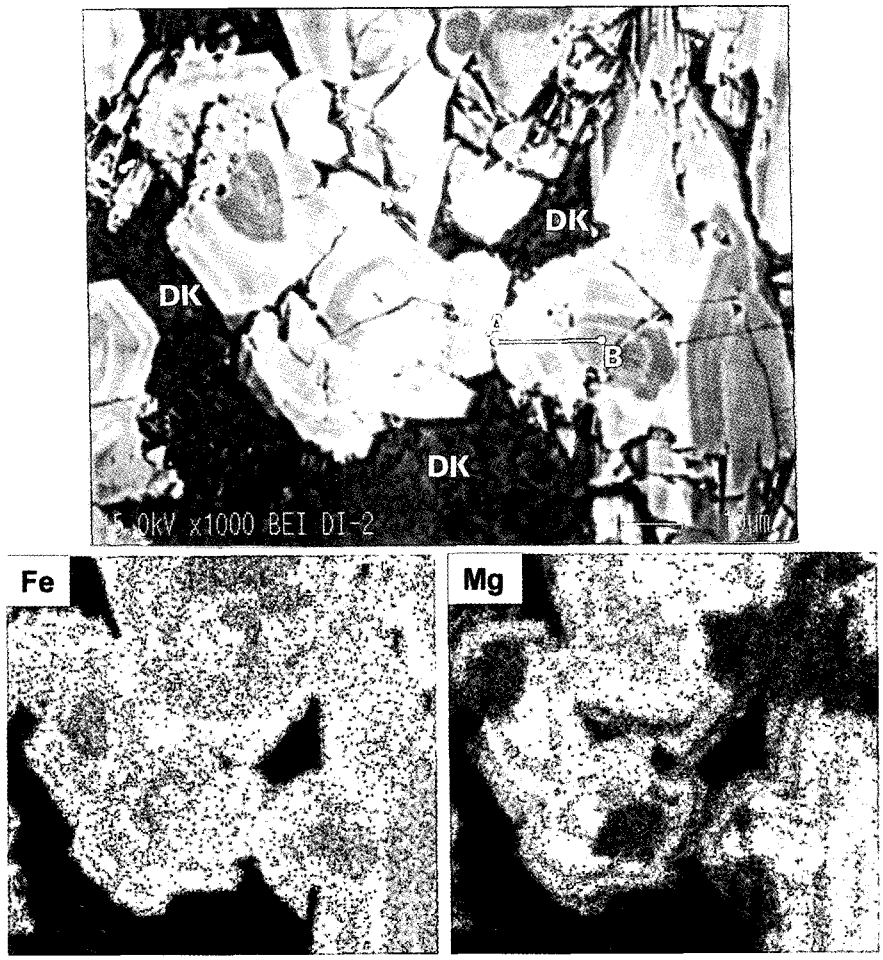

Fig. 3. BSE image and X-ray compositional maps of oscillatory zoned tourmaline. X-ray maps show that Mg is enriched in the core, whereas Fe is enriched in the rim, consistent with the compositional contrast of the BSE image. Note tourmaline partially altered by dickite (DK). Scale of the BSE image is 10 μm.

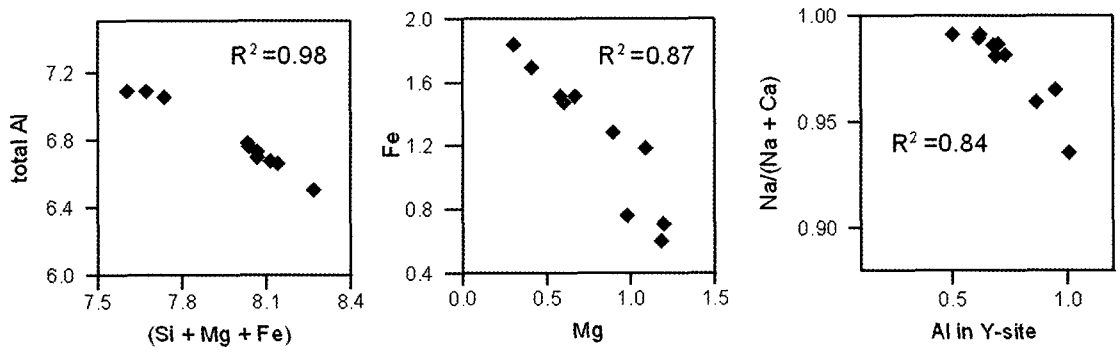

Fig. 4. Correlation between some components represented by determinative coefficients (R squares). (a) Plot of the sum of (Si + Mg + Fe) vs. total Al. (b) Plot of Mg vs. Fe. (c) Plot of Al in the Y site vs. the ratio Na/(Na + Ca).

weak fluctuations and an abrupt decrease near the core, though negligible across the zoning.

DISCUSSION

The oscillatory zoning in tourmaline reveals alternation of Fe-rich and Mg-rich zones, which reflects either changes in the activity ratio of Fe/Mg, or changes in the distribution of Fe and Mg between fluid and tourmaline during the alteration processes. Inasmuch as tourmaline possesses fine-scale zonation such as oscillatory zoning, it crystallized in an environment where physical and chemical properties fluctuated rapidly. The solubility of tourmaline is the principal control on the B content of peraluminous magmas and the activity of aluminum in melt appears to be among the important parameters for tourmaline stability and requires a higher total concentration of Al to promote tourmaline growth (London *et al.*, 1996; London, 1999). Formation of the tourmaline and may have involved leaching of Al from silicate wall rocks under high water/rock conditions in order to precipitate these aluminous minerals (Slack, 1996). The fact that tourmaline altered to diaspore and dickite at the marginal part of the crystal indicates that tourmaline tended to be unstable with respect to these aluminous minerals with decreasing boron activity. Since tourmaline is unstable in fluids with pH > 6.5, and in system having low Fe-Mg contents, breakdown of tourmaline reflects the incursion of high pH and boron-undersaturated fluids (Morgan and London, 1989).

Because the diaspore nodule occur at the limited area where fracturing develops, the development of oscillatory zoning indicates an open system with a continuous or discontinuous mass flux into or through the region in which crystal growth take place. Such a zone is favorable to act as an indication of infiltration metasomatism (Yardley *et al.*, 1991; London and Manning, 1995). Such an open system behavior requires that the B source to form tourmaline is external to metasomatic. Tin-minerals, dumortierite, tourmaline, molybdenite, and wolframite are commonly found in the pegmatite or quartz veins of the biotite granite adjacent to the andesitis tuff (Hong and Choi, 1988). Therefore, the magma from which biotite granite crystallized was the most possible sources of boron necessary to form tourmaline in the diaspore nodule. Alteration of the andesitic tuff around the deposit took place along fracture zones that might act as channels for acid solutions derived from adjacent biotite granite. In diaspore nodules anatase is commonly present, but no micas are found. Competition with biotite seems to be a crucial parameter for controlling the stability of tourmaline (Bernard *et al.*, 1985; Wilke *et al.*, 2002). Since there is lack of competition for Fe and Mg between mafic minerals such as biotite, tourmaline could be free to crystallize in the diaspore nodules during the earlier stage. Therefore, it is reasonable to conclude that the Fe-Mg contents in the hydrothermal fluids were not so high enough to form mafic minerals except Fe-Mg tourmalines. The fact that diaspore nodules containing tourmaline also possess TiO_2 mineral suggests that tourmaline does not accept all of the Fe in its structure, as observed in the synthetic tourmaline by Fuchs *et al.* (1998). After consuming up of Fe and Mg for tourmaline, aluminum-rich minerals formed with decreasing the boron activity. In summary, boron, together with and Fe and Mg, was consumed by the crystallization of tourmaline and alkali- free compositions seemed favorable to form tourmaline.

CONCLUSIONS

The fine-scale chemical zonation of hydrothermal tourmaline reflects the fluctuation conditions that would be expected from fluid mixing in open systems. Oscillatory chemical zoning in tourmaline formed and showed similar patterns, regardless of its crystallographic directions. Mg was enriched in the early stage of crystal growth while Fe was enriched in the later stage, with fluctuations of the ratio of Fe to Mg. The boron content has little effect on development of the oscillatory zoning. Boron, together with and Fe and Mg, was consumed by the crystallization of tourmaline and alkali-free compositions except trace Na seemed also favorable to

form tourmaline. Tourmaline became to be unstable with respect to aluminous minerals such as diaspore and dickite. Tourmaline could be free to crystallize in the diaspore nodules during the earlier stage and the Fe-Mg contents in the hydrothermal fluids were not so high enough to form mafic minerals except Fe-Mg tourmaline. Tourmaline was unstable with respect to these aluminous minerals as the B, Fe, and Mg activities decreased. The aluminum activity may control the stability of tourmaline in the hydrothermal system.

ACKNOWLEDGEMENTS

This study was supported by Korea Science and Engineering Foundation R05-2002-000-00898-0 granted to Kim, Y. Instrumental analyses were carried out at the Korea Basic Sciences Institute (KBSI) and Kyungpook Center for Scientific Instruments at KNU.

REFERENCES

Bernard, F., Moutou, P., and Pichavant, M. (1985) Phase elations of tourmaline leucogranites and the significance of tourmaline in silicic magmas. J. Geol., 93, 271-291.

Cavaretta, G. and Puxedda, M. (1990) Schorl-dravite-ferridravite tourmalines deposited by hydrothemal magmatic fluids during early evolution of the Larderello geothermal field, Italy. Econ. Geol., 85, 1236-1251.

Choo, C.O., Kim, J.J., and Kim, Y. (2001) Complex zoned tourmaline in the diaspore nodule from a hydrothermal kaolin deposit, Miryang, south Korea. 11st Annual Goldschmidt Conference, Program, 147.

Choo, C.O. and Kim. Y. (2003) Textural and spectroscopic studies on hydrothermal dumortierite from an Al-rich clay deposit, southeastern Korea. Mineral. Mag., 67, 799-806.

Dutrow, B.L. and Henry, D.J. (2000) Complexly zoned fibrous tourmaline, Cruzeiro mine, Minas Gerais, Brazil: A record of evolving magmatic and hydrothermal fluids. Can. Mineral., 38, 131-143.

Fuchs, Y., Lagache, M., and Linares, J. (1998) Fe-tourmaline synthesis under different T and fO_2 conditions. Am. Mineral., 83, 525-534.

Henry, D.J. and Dutrow, B.L. (1996) Metamorphic tourmaline and its petrologic applications. Rev. Mineral., 33, 500-555.

Henry. D.J., Kirkland, B.L., and Kirkland, D.W. (1999) Sector-zoned tourmaline from the cap rock of a salt dome. Eur. J. Mineral., 11, 263-280.

Hong, S.H. and Choi, P.Y. (1988) Geological report of the Yuchon sheet. Korea Institute of Energy and Resources, 1-26.

Hwang, S.K. and Kim, S.W. (1994) Petrology of Cretaceous volcanic rocks in the Milyang-Yangsan area, Korea (I): Petrotectonic setting. Jour. Geol. Soc. Korea, 30, 229-241.

Jin, M.S., Kim, S.J., and Shin, S.C. (1991) Fission track and K-Ar ages of granites in the southeastern Korea. Korea Inst. Geol. Mining KR., 90-1B2, 57-98.

Kim. S.J., Kim, J.J., and Choo, C.O. (1992) Mineralogy and genesis of hydrothermal deposits in the southeastern part of Korean peninsula: (3) Miryang napseok deposit. Jour. Mineral. Soc. Korea, 5, 93-101.

Koh, S.M., Tagaki, T., Kim, M.Y., Naito, K., Hong, S.S., and Sudo, S. (2000) Geological and geochemical characteristics of the hydrothermal clay alteration in south Korea. Resource Geol., 50, 229-242.

Lee, K., Moo, H.-S., Song, Y., and Kim, I.J. (1993) Wall rock alteration and genetic environment of the Milyrang pyrophyllite deposit. Jour. Korean Inst. Mining Geol., 26, 289-309.

London, D. and Manning, D.C. (1995) Chemical variation and significance of tourmaline from southwest England. Econ. Geol., 90, 495-519.

London, D., Morgan, G.V., and Wolf, M.B. (1996) Boron in granitic rocks and their contact aureoles. Rev. Mineral., 33, 299-330.

London, D. (1999) Stability of tourmaline in peraluminous granite systems: the boron cycle from anatexis to hydrothermal aureoles. Eur. Jour. Mineral., 11, 253-262.

Michailidis, K., Kassoli-Fournaraki, A., and Dietrich, R. V. (1996) Origin of zoned tourmalines in graphite-rich metasedimentary rocks from Macedonia, northern Greece. Eur. J. Mineral., 8, 393-404.

Min, K.D., Kim, O.J., Lee, D.S., and Choo, S.H. (1982) Applicability of plate tectonics to the post Late Cretaceous igneous activities and mineralization in outhern part of South Korea(I). Jour. Korea Inst. Mining. Geol., 15, 123-154.

Morgan, G.B., VI and London, D. (1989) Experimental reactions of amphibolite with boron-bearing aqueous fluids at 200 MPa: Implications for tourmaline stability and partial melting in mafic rocks. Contrib. Mineral. Petrol., 102, 281-297.

Nieva, A.M.R. (1974) Geochemistry of tourmaline (schorlite)

from granites, aplites, and pegmatites from northern Portugal. Geochim. Cosmochim. Acta, 38, 1307-1317.

Papezik, V.S. and Keats, H.F. (1976) Diaspore in a pyrophyllite deposit on the Avalon peninsula, Newfoundland. Can. Mineral., 14, 442-449.

Power, G.M. (1968) Chemical variation in tourmalines from southwest England. Mineral. Mag., 36, 1078-1089.

Shore, M. and Fowler, A.D. (1996) Oscillatory zoning in minerals: a common phenomenon. Can. Mineral., 43, 1111-1126.

Slack, J.F. (1996) Tourmaline associations with hydrothermal ore deposits. Rev. Mineral., 33, 559-643.

Taylor, B.E. and Slack, J.F.(1984) Tourmalines from Appalachian-Caledonian massive sulfide deposits: textural, chemical and isotopic relationships. Econ. Geol., 79, 1703-1726.

Werding, G. and Schreyer, W. (1996) Experimental studies on borosilicates and selected borates. Rev. Mineral., 33, 118-163.

Wilke, M., Nabelek, P.I., and Glascock, M.D. (2002): B and Li in Proterozoic metapelites from the Black Hills, U.S.A.: Implications for the origin of leucogranitic magmas. Am. Mineral., 87, 491-500.

Yardley, B.W.D., Rochelle, C.A., Barnicoat, A.C., and Lloyd, G.E. (1991) Oscillatory zoning in metamorphic minerals: an indicator of infiltration metasomatism. Mineral. Mag., 55, 357-365.

2005년 9월 5일 원고접수, 2005년 9월 20일 게재승인.